Computers and Concrete, Vol. 6, No. 1 (2009) 41-57
DOI: http://dx.doi.org/10.12989/cac.2009.6.1.041

Experimental, numerical and analytical studies on a novel external prestressing technique for concrete structural components

N. Lakshmanan[†], S. Saibabu[‡], A. Rama Chandra Murthy[‡†], S. Chitra Ganapathi[‡†] and R. Jayaraman[‡†]

SERC, CSIR, CSIR Campus, Taramani, Chennai, 600-113, India

R. Senthil[‡‡]

Structural Engineering Department, Anna University, Chennai-34, India

(Received February 20, 2008, Accepted February 4, 2009)

Abstract. This paper presents the details of a novel external prestressing technique for strengthening of concrete members. In the proposed technique, transfer of external force is in shear mode on the end block thus creating a complex stress distribution and the required transverse prestressing force is lesser compared to conventional techniques. Steel brackets are provided on either side of the end block for transferring external prestressing force and these are connected to the anchor blocks by expansion type anchor bolts. In order to validate the technique, an experimental investigation has been carried out on post-tensioned end blocks. Performance of the end blocks have been studied for design, cracking and ultimate loads. Slip and slope of steel bracket have been recorded at various stages during the experiment. Finite element analysis has been carried out by simulating the test conditions and the responses have been compared. From the analysis, it has been observed that the computed slope and slip of the steel bracket are in good agreement with the corresponding experimental observations. A simplified analytical model has been proposed to compute load-deformation of the loaded steel bracket with respect to the end block. Yield and ultimate loads have been arrived at based on force/moment equilibrium equations at critical sections. Deformation analysis has been carried out based on the assumption that the ratio of axial deformation to vertical deformation of anchor bolt would follow the same ratio at the corresponding forces such as yield and ultimate. It is observed that the computed forces, slip and slopes are in good agreement with the corresponding experimental observations.

Keywords : prestressed concrete; external prestressing; finite element analysis; analytical model; material nonlinearity; slope; slip.

1. Introduction

External prestressing technique is widely used in the new construction of various engineering structures and also as one of the most efficient approaches for strengthening of existing structures.

† Director
‡ Scientist, Corresponding author, E-mail: murthyarc@sercm.org
‡† Scientist
‡‡ Associate Professor

In an external prestressing system, the prestressing tendons are placed outside the concrete section and the prestressing force is transferred to concrete through end anchorages and deviators. External prestressing system is simple to construct and easy to inspect and maintain as compared to the internal tendon system. Many bridges which were designed for earlier loading standards or which have suffered damage or deterioration are not functioning properly for the present traffic conditions. Poor reinforcement detailing, design errors and general wear and tear can impair structural performance. Corrosion of reinforcement, attack by chemicals or pollution, over loading, impact damage from vehicles etc., can lead to loss of strength and loss of prestress. Bridge strengthening by external prestressing is to be carried out to regain the prestress lost. External prestressing technique is being widely used for enhancing strength of the existing/distressed prestressed concrete girders to carry the required loading or enhanced loading. If end blocks are not strong enough to withstand the additional prestressing forces due to the proposed external prestressing, it is susceptible to distress. A physical concept of state of stress in the anchorage zone in the transverse direction, that is, normal to planes parallel with the top and bottom surfaces of the beam is tensile in nature over a length of end block due to internal prestressing at single point. Understanding this state of stress in external prestress is a complex phenomenon.

Many experimental studies on the behaviour of externally prestressed members have been conducted (Ma *et al.* 1999, Aparicio *et al*. 2000, Miyamoto 2000, Aparicio *et al.* 2002, Choy *et al.* 2002, Choy 2005, Lou and Xiang 2006, Czaderski and Motavalli 2007), whereas limited numerical analyses and analytical studies of these structures have been carried out.

Ma *et al*. (1999) provided the details of optimized anchorage zone based on analytical and full-scale experimental studies. Aparicio *et al.* (2000) conducted ultimate load analysis with a nonlinear finite element numerical model and measured the thermal stresses and calculated at the anchorage diaphragms due to the hydration heat of concrete. Miyamoto *et al.* (2000) investigated the dynamic behaviour of prestressed composite girder bridges, strengthened with external tendons. Aparicio *et al*. (2002) presented the results of fibre monolithic and three segmental beams tested in bending and in combined bending and shear. Choy *et al.* (2005) studied the shear transfer mechanism of prestressed concrete encased steel beams. Chen (2005) conducted experiments on four groups of prestressed steel-concrete composite beams with external tendons in negative moment regions. Lou and Xiang (2006) proposed a numerical model based on finite element method incorporating an arc length solution algorithm for materially and geometrically nonlinear analysis of concrete beams prestressed with external tendons. Results predicted by the analysis were in good agreement with the experimental observations. Czaderski and Motavalli (2007) presented details of 40 year old full scale concrete bridge girder with prestressed carbon fibre reinforced polymer plates anchored using gradient method. McNeff (1999) presented analytical method for calculation of moment resistance in anchor bolt connection based on a concrete beam/column analogy. Bahaari and Shebourne (2000) developed a finite element methodology using ANSYS finite element code for equivalent three-dimensional analysis to investigate the behaviour of bolted end-plate connections. Fanning *et al.* (2000) presented an ANSYS finite element model for flush end-plate joints. Material nonlinearity, large deflection analysis and contact surfaces were included in a non-linear solution. Jung *et al.* (2006) presented experimental and finite element investigations of the load-deformation behaviour of tapered steel and fiber-reinforced plastic bridge camera poles subjected to cantilever bending type loading. Kim *et al.* (2007) described finite element analysis and modeling of structure with bolted joint using ANSYS.

1.1. Research significance

In strengthening prestressed concrete beams by external prestressing, the external tendons are generally anchored to the ends of the girder if the end regions are accessible for anchoring. In this method, the external force is transferred to the member in the compression mode. This method is not suitable for strengthening continuous span bridges and suspended span bridges. Steel brackets with through-bolt along with laterally prestressed anchor system is the another method to anchor external prestressing tendons to the end block/web. This technique is widely employed in the field for retrofitting of prestressed concrete (PSC) girders. In this method, transfer of prestress to the member takes place through friction. In this case, the transverse prestressing system may foul with the existing tendons. However bridges, that have been constructed in earlier years did not envisage the need for "strengthening", primarily to compensate excessive loss of prestress. At the ends of the girders there is insufficient space to carry out external prestressing operations later on. As the depth of expansion type anchor bolts are less, they may not reach the level of existing tendons. This method is more suitable to anchor at the ends/webs of simply supported, continuous and suspended spans.

Authors propose a novel technique of side steel bracket with shear key anchors, steel brackets are attached to the sides of the end block of the girders through torque-controlled expansion type anchor bolts. Expansion anchors transfer the tensile loads to the concrete principally by friction at end and transfer the shear load to the concrete by shear. This method has advantage of not requiring lateral/transverse prestressing as necessary in case of conventional method and more suitable where ends of girders are not accessible for anchoring external prestressing. The deviators required for changing the profile of external tendons can be easily constructed with steel brackets, bolted to the existing girder by expansive type anchor bolts which act as effective shear keys in transferring prestress.

Many experiments have been conducted to study the behaviour of end block with varying internal prestressing. To understand behaviour of the anchorage with bolts, with different dia of bolts, with and without internal prestress and with concentric and eccentric external prestressing, five end blocks were fabricated.

End blocks (EB-1, EB-2, EB-3 and EB-5) were tested with 16mm dia bolts. End block (EB-4) was tested with 10 mm dia bolts. Concentric internal prestress force was applied for EB-1, EB-3, EB-4 and EB-5. Specimen EB-2 was tested without internal prestress force. Concentric external load was applied to the specimens EB-1, EB-2, EB-3 and EB-4. Specimen EB-5 was tested with eccentric external load.

Finite element analysis has been carried out and the results are shown for EB-1. Experimental

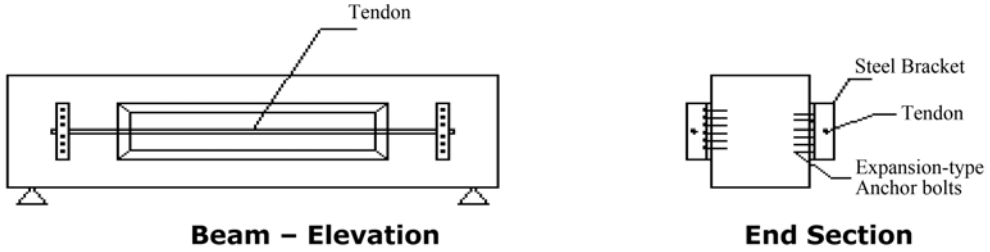

Fig. 1. Anchoring of external prestressing at the sides using expansion - type anchor bolts

details and results pertaining to EB-1 and EB-4 are discussed in the subsequent sections. Simplified analytical model has been proposed and comparison has been made.

2. Prestressed concrete end block

A post-tensioned 'I' beam of effective span 5000 mm with M45 concrete grade is designed which is one-fifth model of prototype girder. The design stresses at transfer and working of model to approximately equal to stress of prototype. The depth of the beam is 650 mm and flange width at top and bottom is 200 mm. Flange thicknesses at top and bottom are 90 mm and thickness of web is 120 mm. Research area is concentrated only at the anchorage zone of external prestressing, hence end section of I-girder of length 1020 mm consisting of a rectangular portion of 700 mm and an I-shaped segment of 320 mm is chosen as the test specimens. Details of reinforcement of the test specimen are shown in Fig. 2.

Concrete of grade 45MPa is used to cast end block specimens. The proportion of concrete ingredients obtained as per design-mix to achieve the target compressive strength of 45 MPa is 1:1.83:2.74 and water cement ratio is 0.4. The cement used in the mix is 53-grade ordinary portland

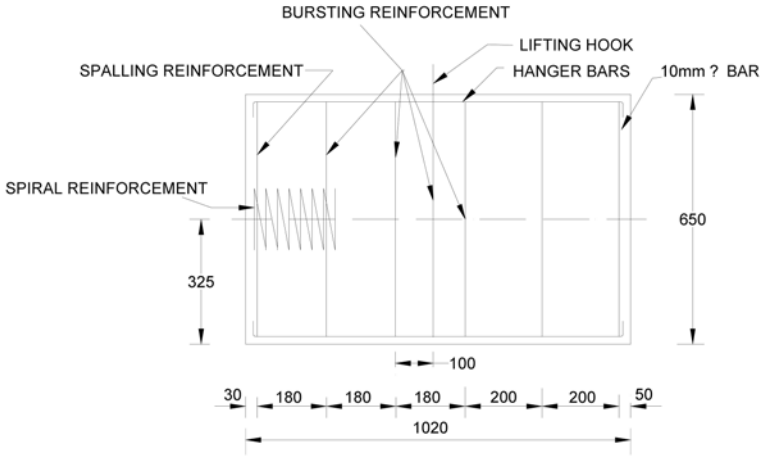

Fig. 2 Reinforcement details of end block

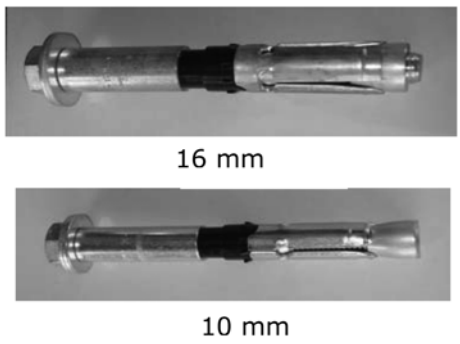

Fig. 3 Torque-controlled expansion anchors

cement. High-yield strength deformed bars having yield strength of 415 N/mm^2 are used as reinforcement. The high tensile rock-anchor rod of 36 mm dia. having an average tensile strength of 1000 MPa is used for applying simulated internal prestressing force of 624 kN to the test specimen. Higher shear strength expansion type anchor bolts having design shear strength of 80.9 kN and tensile strength of 33.6 kN are used for transferring external prestressing force to the concrete member in shear mode. Two types of expansion type anchors are used in the tests and are shown in Fig. 3. These are used in the design for anchoring the external prestress of 188 kN accounting 30% loss of initial prestress.

2.1. Instrumentation

To measure out-of-plane displacement and vertical displacement of the bracket, dial gauges, D1, D2…. are positioned. Positions of dial gauges are shown on the development surface of end block in Fig. 4. To measure vertical displacement (slip) of bracket during external prestressing, dial gauges are positioned parallel to the end block, one at the top of steel bracket and other on the concrete at the same level. To measure out-of-plane displacement (to compute slope) of bracket during external prestressing, dial gauges are positioned perpendicular to the end block, one at the

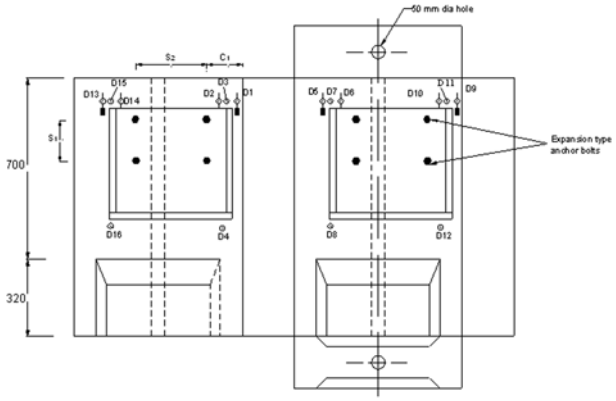

Fig. 4 Instrumentation details

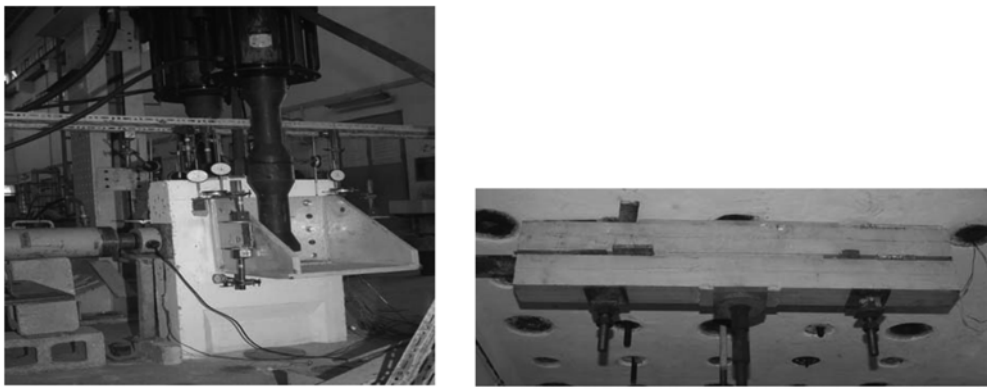

(a) Test specimen above the test floor (b) Below the test floor

Fig. 5 Test set-up

top of steel bracket and other bottom of steel bracket at each corner of steel bracket. Dial gauges have a least count of 0.01 mm.

2.2. Test setup

Two rigid steel brackets are designed to transfer the external prestressing force on to the test specimen. These brackets are connected to the test specimen by expansion type anchor bolts. Two hydraulic actuators are fixed to the loading frame to apply external force on the steel brackets. The test specimen itself is anchored to the test floor through a system of box beams and high strength bolts. The calculated reaction at the support of beam is applied to the test specimen through a horizontal jack. The horizontal jack is fixed to rigid pedestal anchored to the test floor. The vertical load simulating the external prestress through two vertical actuators is controlled from a hydraulic loading plant, while the horizontal jack simulating the support reaction on the beam is controlled through a separate electrically operated pump. Test set-up including test floor is shown in Fig. 5.

2.3. Test procedure

Internal full prestress force of 625 kN is applied vertically by tensioning 36 mm dia. anchor rod against the test floor. End reaction component of 125 kN corresponding to the design live load acting on the beam is applied horizontally through 300 kN capacity jack. For test specimen of 16mm dia bolts , holes of 25 mm dia and 125 mm long are drilled on each side of end block at four locations to insert expansion type bolts of 16 mm dia. Four bolts are arranged at an effective horizontal spacing of 275 mm and vertical spacing of 160 mm on each side of the specimen. The effective minimum edge distance provided for the bolts is 140 mm. Positions of expansion type anchor bolts are identified with symbol '●' in Fig. 4. The bolts were inserted through the steel brackets on both sides and tightened by a torque-meter to specified value of 120 N-m. The effective anchorage depth, designed tensile and shear loads of single bolt are 120 mm, 33.6 kN and 80.9 kN respectively. External prestress is applied as a vertical load on steel brackets in increments of 15 kN per actuator. For the case of EB-1, reaction load is kept constant whereas reaction load is varied proportional to the external load for the other test specimens. The loads are applied till failure of the end blocks. Corresponding to each stage of loading, the dial gauge readings are recorded. During application of external load, rotation as well as slipping of steel bracket against the concrete is measured.

2.4. Discussion of test results

First visible crack is observed on the top surface of the specimen which extended through out the width of the specimen for EB-1. The corresponding load is 540 kN. Formation of crack indicates that the development of tension in the concrete above the top row bolts due to bending action caused by the external loads. With further increase in load, the same crack propagated vertically on either of the vertical surfaces. Further, inclined cracks are observed originating from the top row of the bolts propagating away from the bolt towards the nearest edges of the specimen. With further increase in external load, cracks started on both vertical faces of the specimen and widening the already formed cracks. Pullout failure of the bolts along with concrete surrounding bolts and concrete edge failure occurred simultaneously at ultimate load. The ultimate load for EB-1 is 795 kN.

Fig. 6 Failure pattern of EB-1 at ultimate load

Fig. 7 Failure pattern of EB-4 at ultimate load

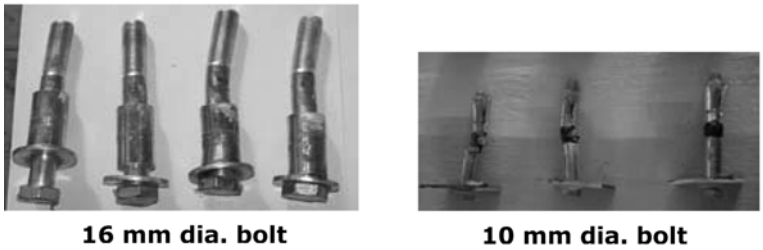

Fig. 8 Deformed shape of bolts

Failure pattern of specimen (EB-1) at ultimate load is shown in Fig. 6. Design load for the group of 16mm dia. bolts is 245 kN. The ratio of ultimate load and cracking load is 1.47 whereas the ratio of ultimate load and design load is 3.25. First visible crack is observed on the surface of the specimen for EB-4 and the corresponding load is 320 kN. The reason for early cracks in EB-4 is attributed to smaller dia. of bolts, less anchorage depth of bolts and concrete surrounding bolts is subjected to more tension. The ultimate load for EB-4 is 570 kN. At ultimate load, concrete surrounding the bolts is pulled out suddenly due to increase in tension more than the concrete cone capacity. Fig. 7 shows the failure pattern of EB-4. Design load for the group of 10 mm dia. bolts is 252 kN. The ratio of ultimate load and cracking load is 1.78 whereas the ratio of ultimate load and design load is 2.26. Deformation of the bolt in EB-1 and EB-4 at ultimate load is shown in Fig. 8. A ductile failure is observed in EB-1 where as a sudden failure is observed in EB-4. Spalling and crushing of concrete are observed more in EB-1 than in EB-4 at failure. At ultimate load, EB-1 performed better than EB-4.

2.4. Slips and slopes

Slips (vertical deformation) and slopes (horizontal deformation) of steel bracket are important observation as they indicate loss of external prestress. The behaviour of the EB-1 and EB-4 is similar upto design load. The average slip of EB-1 and EB-4 is 0.3 mm at their respective design loads. The average slip of EB-1 at cracking load and ultimate loads are 4.6 mm and 11.08 mm respectively, while the corresponding values of slip for EB-4 are 3.0 mm and 9.87 mm respectively. It can be observed that the slip is lesser by 30% and 50% at cracking load and ultimate load respectively in the case of EB-1 compared to that of EB-4. The reason may be due to more

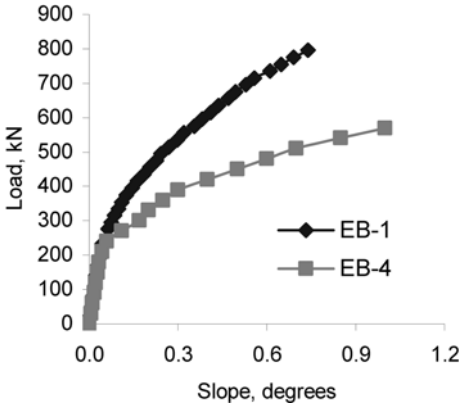

Fig. 9 Slope of the steel bracket

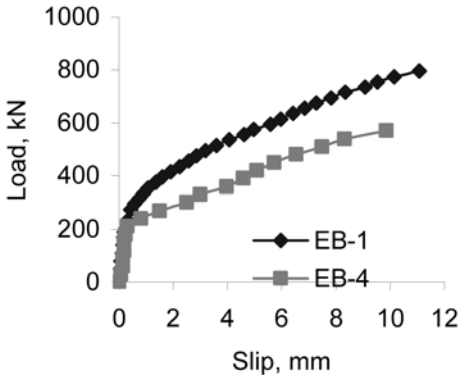

Fig. 10 Slip of the steel bracket

anchorage depth. Slope is calculated using the measured out-of-plane deformation. Slope of the steel bracket at ultimate loads for EB-1 and EB-4 are 0.74° and 1.0° respectively. It can be observed that the slope is lesser by 50% and 36% at cracking load and ultimate load respectively in the case of EB-1 compared to that of EB-4. It can be observed that slope of EB-4 is more than the value that of EB-1 at a given load. Slope and slip of the steel bracket under combination of loads for test specimens EB-1 and EB-4 are shown in Fig. 9 and Fig. 10 respectively.

3. Finite element modelling and analysis

Finite element analysis (FEA) is a numerical technique, widely employed to the structures/ structural components. FEA is a tool that can simulate and predict the responses of reinforced and prestressed concrete members. Finite element modeling and analysis is carried out by simulating the testing conditions of EB-1 and EB-4. Popular finite element software ANSYS has been used for modeling and analysis of the end block with anchor bolts ANSYS 6.0 (2002). Details of results of analysis pertaining to EB-1 are provided herein.

3.1. Finite element modelling issues

A large number of different FE formulations have been used for the analysis of concrete structural components. These may be categorized into facet plate/shell elements, thin-shell elements (Kirchoff assumptions), thin/thick shell elements (Reissner-Mindlin theory) and three dimensional elements. The choice of an element for analysis of a structure/component depends on the geometry and the purpose for which the results of the analysis are to be used. The following are some of the key issues w.r.t modelling of PSC end block.

- FE modelling of post tensioned prestressed concrete end block
- FE modelling of steel bracket and expansive type anchor bolts
- Material modelling of concrete, steel and bolt
- Modelling of various loads such as compression load, reaction load on end block, pretension in the bolt and external load on steel bracket.
- Simulation of initial pretension and equivalent compression in concrete surrounding the bolt

- Modelling end connections such as bolt and steel bracket and bolt and concrete block
- Employing appropriate element types such as contact, gap, solid and link for effective load transfer and to simulate the realistic behaviour
- Simulation of material nonlinearity for larger load steps and cracked concrete behaviour.

3.2. FE modeling and analysis of EB-1

Volume has been created as per the geometry described in section 2. Eight noded solid elements (SOLID 45) have been employed to model concrete block, bolts and bracket connection. The use of these elements provides the same number of integration point density as the higher order elements but requires much less computational effort. This element is defined by orthotropic material properties that correspond to the element coordinate directions. Each node has three translational degrees of freedom, namely, Ux, Uy and Uz in x, y and z directions respectively. The element has plasticity, creep, swelling, stress stiffening, large deflection, and large strain capabilities. Bolt is idealized as square in shape instead of circular to avoid modeling issues. The bolt is embedded for a length of 125 mm inside the concrete block. At the end of the bolt, a link element has been created connecting the surfaces of bolt and concrete. The principal function of link element is to transfer the forces arising due to external prestressing loads. An imaginary surface has been created between the concrete block and the bracket in order to allow the bolt movement in the out of plane direction under the external prestressing load.

3.2.1. Material properties

The following are the material properties considered for the concrete, steel and bolt. For linear static analysis, modulus of elasticity, poisson's ratio are the input whereas for nonlinear static analysis, multilinear elastic model available in ANSYS has been used. The material behavior in multilinear elastic model is described by a piece-wise linear stress-strain curve. Fig. 11 shows multilinear stress strain plot adopted for steel and concrete material.

Material	Modulus of elasticity, MPa	Poissons'ratio, ν
Concrete	31623	0.12
Steel	2×10^5	0.3
Bolt	2×10^5	0.3

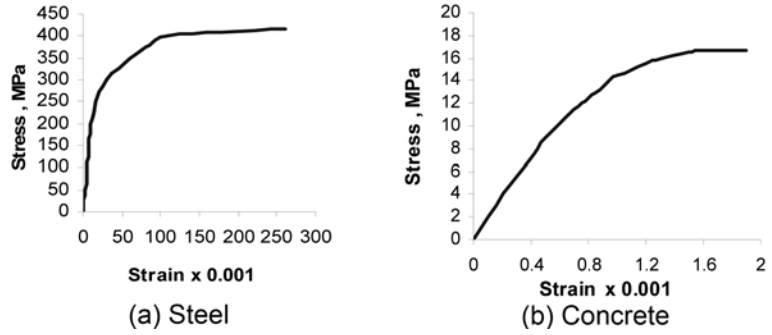

Fig. 11. Multi-linear stress-strain plot

3.2.2. Loading conditions

As already stated, there are various loadings, namely shear load in the form of reaction, pretension in the bolt, initial prestress and external prestress. Initial prestress is applied as compressive load on the top of the PSC block. Initial pretension force obtained by applying torque on the bolt, is applied to all the bolts on the face of the element and an equivalent compressive force is applied to all the surrounding elements of the bolt to simulate the head of the bolt. It is assumed that there is prefect frictional bond between bolt and concrete. Shear load, prestress load on the block and initial pretension to the bolt are maintained same throughout the analysis. External prestressing load is applied incrementally on the projection part of the bracket to capture nonlinearities induced by material yielding at larger load. The magnitudes of the loads are given below.

Reaction load (to PSC block)	:	125 kN
Prestress load (on concrete block)	:	438 kN
Initial pretension (to each bolt)	:	37.5 kN
External prestress load (on bracket)	:	0 to 400 kN

3.2.3. Boundary conditions

All the degree of freedom, have been constrained on the bottom surface of the block simulating the fixity condition of test floor.

FE mesh along with modeling characteristics is shown in Fig. 12.

Linear static and nonlinear static analysis have been carried out depending on the magnitude of external prestressing load. At each incremental load, out-of-plane deformation and slip have been noted down. Rotation of the bracket has been calculated by using the computed out-of-plane deformation. Figs. 13 and 14 show the out-of-plane deformation and vertical deformation (slip) respectively upto an ultimate load of 400 kN. The computed slope and slip values of steel bracket have been compared with the corresponding experimental observations. Figs. 15 and 16 show the slope and slip plots comparing computed and experimental values. From Fig. 15, it can be observed that the computed slopes and the corresponding experimental observations are in very good agreement with each other. From Fig. 16, it

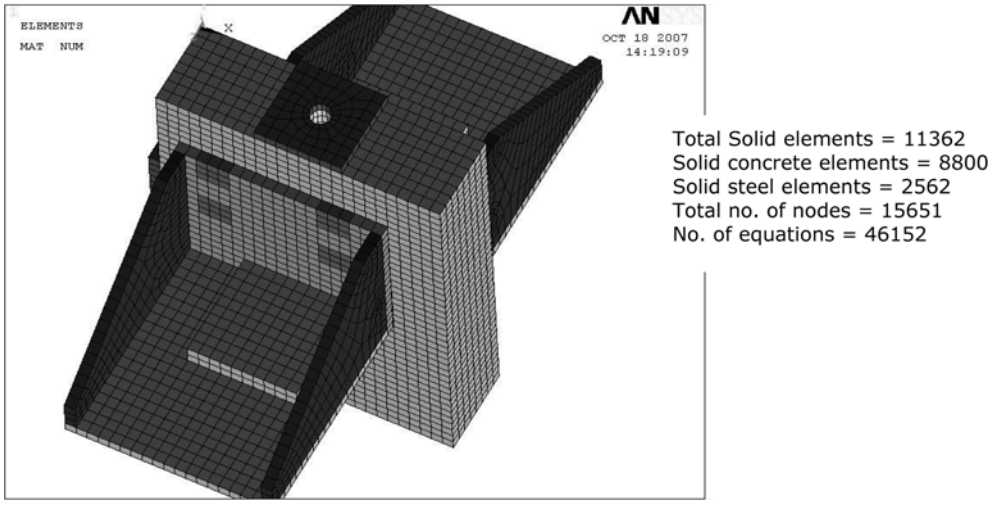

Fig. 12. FE mesh and modeling characteristics

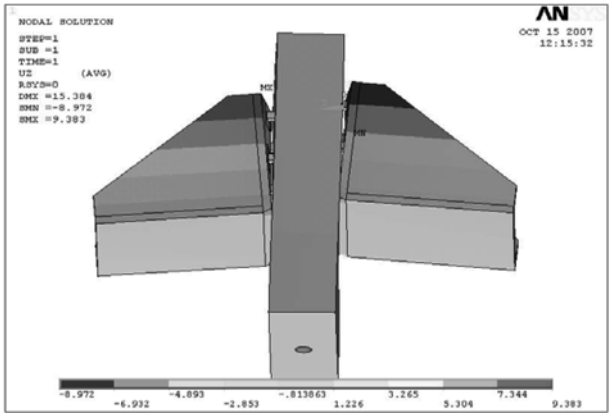

Fig. 13 Out-of-plane deformation at ultimate load

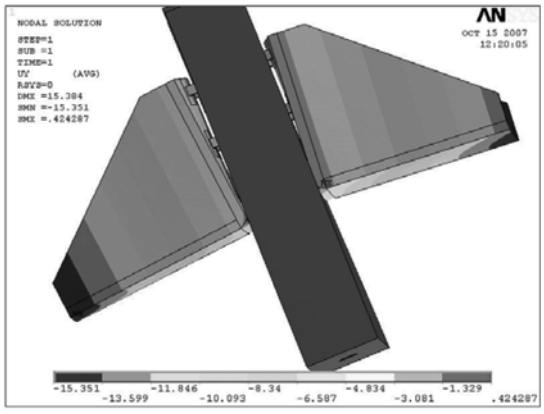

Fig. 14 Vertical deformation (Slip) at ultimate load

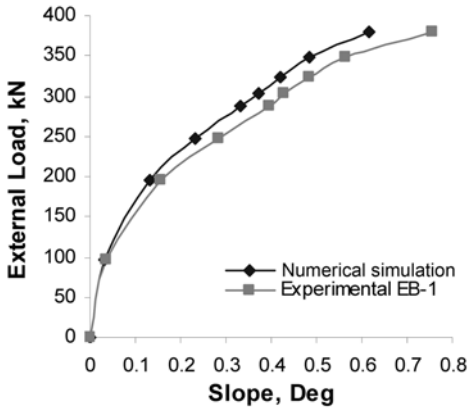

Fig. 15 Slope of Steel bracket under external prestress load for EB-1

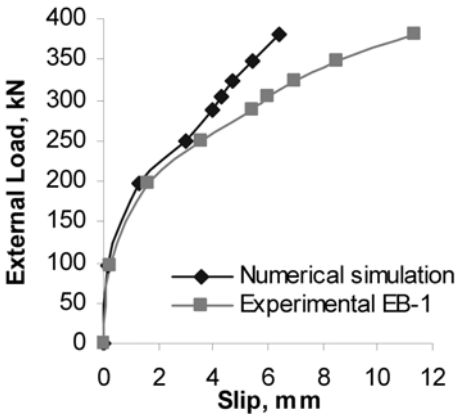

Fig. 16 Slip of Steel bracket under external prestress load for EB-1

can be observed that there is reasonable agreement between the computed and experimental slip values. The difference in the slip may be attributed to the noncoincident of nodal location and experimentally measured point.

4. Behaviour of the joint used for shear anchorage using analytical approach

The behaviour of the joint comprising of a steel bracket and high tensile expansion type anchor bolts is extremely complex. A simplified analytical model is attempted in this section for approximately evaluating the structural load-deformation behaviour of the loaded steel bracket with respect to the end block. The expansion type anchor bolt is firmly anchored to concrete by embedment. The yield and ultimate strengths of the 16 mm dia are 128 kN and 160 kN respectively. Similarly, 10 mm dia. bolt has yield and ultimate load capacities of 50 kN and 62.8 kN respectively.

Hence as a single anchor, concrete failure will not occur. However when the bolts are used in a group, the group anchor capacity is not the same as the sum of the number of bolts in the group.

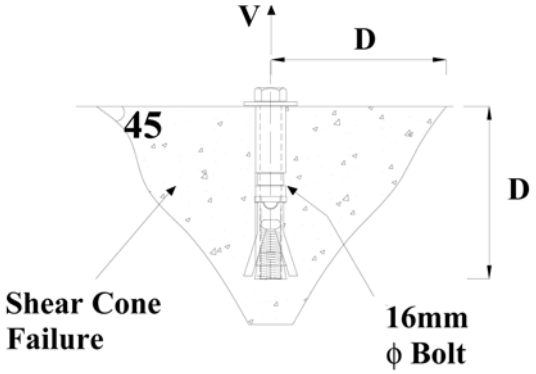

Fig. 17. Pull out capacity of isolated bolt

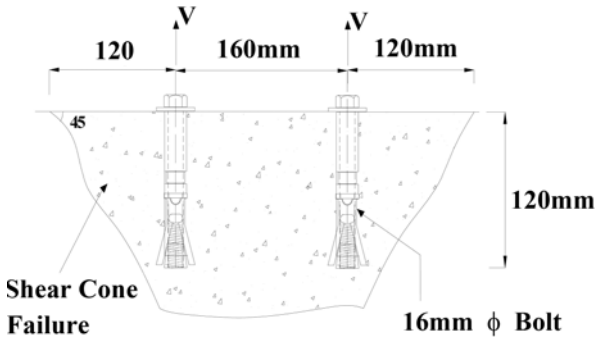

Fig. 18. Interaction of two 16 mm dia. Bolts (EB-1, EB-5)

The 16 mm bolts are spaced at 160 mm vertically and 275 mm horizontally. The 10 mm bolts are spaced at 80 mm vertically and 137.5 mm horizontally. Since the horizontal spacing is more, the bolts in a single vertical line will not interact. However since the vertical separation in less the effective pull out areas will overlap and this would affect the capacity. The pull out capacity of an isolated bolt as shown in Fig. 17.

Component in the vertical direction (V) = $\pi D^2 f_{sp}$ (1)

Where f_{sp} = tensile strength of concrete = 4.0 N/sq.mm

D = embedment length of bolt

The computed V for 16 mm dia bolts of 120 mm embedded length, for single anchor is 180 kN. Fig. 18 shows the interaction among bolts located two in a line for 16 mm dia bolts. The effective embedment depth is 200 mm. The effective pull out force can be computed as 335 kN. For the case EB-4, 3 bolts of 10 mm dia, spaced at 80 mm centers, as shown in Fig. 19, the effective area is 53247 sq.mm. The corresponding computed V is 213 kN.

In this case also failure would be initiated by yielding of steel. The important factor that is to be considered is that the bolts are subjected to shear in addition to axial tension. The experimental programme has clearly revealed rupture of concrete also plays significant role in addition to bending of the anchor bolts at advanced stages of loading. Schematic diagram of anchorage on one side is shown in Fig. 20. From Fig. 20, it can be observed that section 1-1 and 2-2 are critical sections. The anchor block rotates about edge B creating tensile forces in anchor bolts. The bolts also

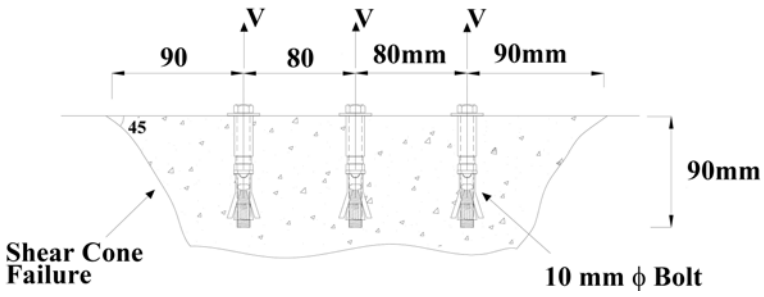

Fig. 19 Interaction of three 10 mm dia. Bolts (EB-4)

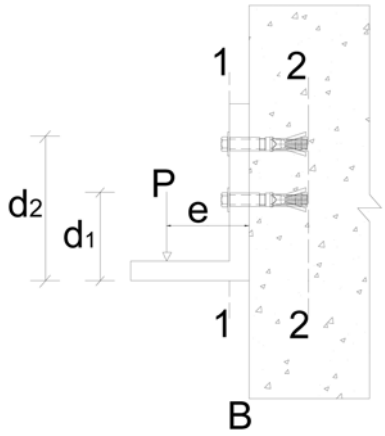

Fig. 20 Schematic Diagram of anchorage

transmit the external load P in shear mode. Hence, at the time of yielding for the configuration used with 16 mm bolts, the distances d_1 and d_2 are 0.28 m and 0.36 m respectively. Assuming the top bolts are yield under combined axial and shear forces due to the external load P. The axial component of load and shear component of load are called F_M and Fs respectively.

$$d_2 F_M + \frac{d_1}{d_2} d_1 F_M = p \cdot e_x \tag{2}$$

Where e_x = position of applied load external P = 120 mm
d_1 = Distance of second row bolts from bottom of bracket=280 mm
d_2 = Distance of first row bolts from bottom of bracket=360 mm

From the Eq. (2) the calculated F_M value is 20.8% of P. The F_S value is assumed as 50% of P. Assuming von-Mises failure criteria

$$(F_M)^2 + 3(F_S)^2 = (F_Y)^2 \tag{3}$$

where, F_y=yield force of bolt.
on solving Eq. (3), P is obtained as 144 kN. Hence loading corresponding to yield stage is 144 kN. The loading is not centrally applied between the bolt lines as can be seen from the experimental set-up. Approximately 2/3 of the load goes to the heavily loaded bolt lines and 1/3 to the other bolt line. Thus the loading on one bracket at the time of yielding of the heavily loaded bolt is 1.5 times the loading on heavily loaded bolt line. Hence the computed pull out force is 215 kN. Beyond the stage of yielding, redistribution of forces can occur due to non-linearity. At the ultimate stage

$$d_2 F_{Mu} + d_1 F_{Mu} = P_u \cdot e_x \tag{4}$$

Using Eq. (4), the calculated F_{MU} is 19% of Pu from the Eq. (4). Hence the value of Pu is 180 kN from the Eq. (3). For two rows, the failure load would be approximately 360 kN.

A similar procedure can be adopted for the 10 mm dia. bolt for EB-4 test specimen with three bolts on each vertical line. Total three vertical lines are arranged at each side of specimen. The yield and ultimate load per bracket can be worked out as 142 kN and 238 kN respectively.

Eccentric external loading on the bracket in the test specimen EB-5 would lead to higher tensile

stresses in plane 2-2. The effect of this increase is found to reduce the loading by about 10 to 12% and can be accounted for by a factor F given by

$$Pe = FP \tag{5}$$

where, Pe = load with eccentric arrangement,

$$F = \frac{1}{(1 + e/B)} \tag{6}$$

where, e = eccentricity to external load = 60 mm
B = overall width of tension anchorage= 575 mm
and P = load without eccentricity.

For the present case, F works out as 0.9.
Hence the yield and failure capacities for EB-5 would be 193 kN and 324 kN per bracket.

4.1. Deformation analysis

It is hypothesized that the ratio of axial deformation to vertical deformation of the anchor bolt would bear the same ratio as the corresponding forces computed at different stages, namely yield and ultimate. Also the resultant deformation would be equal to the deformation corresponding to the pure axial mode. Thus,

$$\frac{\delta v}{\delta x} = \frac{v}{x} \tag{7}$$

$$\sqrt{\delta_v^2 + \delta_x^2} = \delta_a \tag{8}$$

where, v = transverse loading on bolt
x = axial loading on bolt
δ_v = transverse deformation of bolt and
δ_x = axial deformation of the bolt
δ_a = deformation under pure axial loading = length of bolt times ε
ε = The proof strain of high strength bolt, assumed as 0.0052.

δ_x and δ_v are further function of δ_a, where

$$\delta_x = \frac{\delta_a}{\sqrt{3}} \quad \text{and} \quad \delta_v = \sqrt{\frac{2}{3}}\delta_a \tag{9}$$

Hence, at the stage of yielding, for the 16 mm dia. bolt case, the axial deformation and vertical deformation can be computed as 0.45 mm and 0.64 mm respectively and the rotation, θ can be computed as the δ_a divided by d_2. The rotation at yield stage works out to 0.12°. At ultimate stage, the assumed strain is 10% , the vertical deformation is 12.8mm and rotation is 2.4°.

For the 10 mm configuration, at yield, vertical deformation, axial deformation and rotation is 0.47 mm, 0.41 mm and 0.1° respectively. At ultimate stage the computed vertical deformation, axial deformation and rotation is 10.20 mm, 6.0 mm and 1.9° respectively.

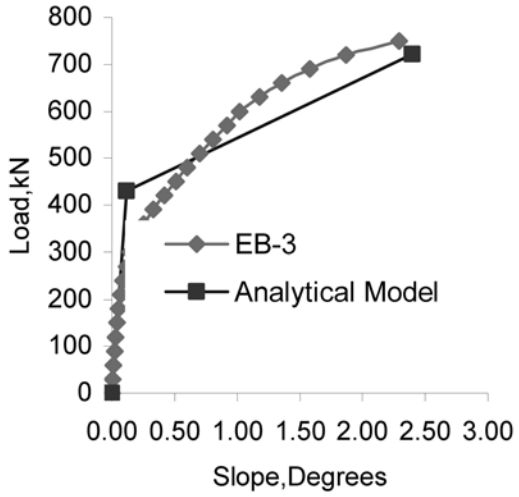

Fig. 21 Slope of the steel bracket during external load for EB-1 and analytical model

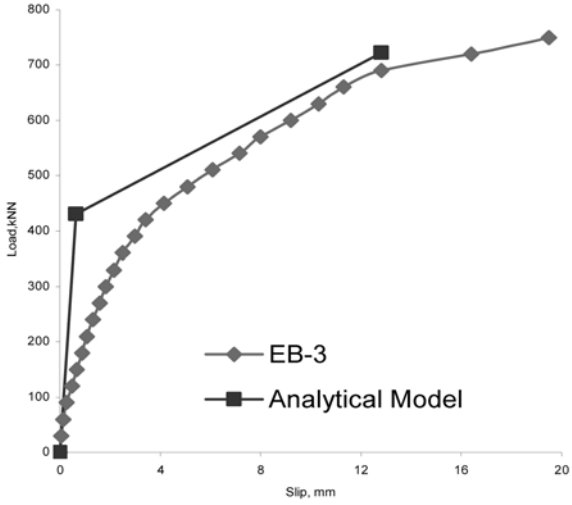

Fig. 22 Slip of the steel bracket during external load for EB-1 and analytical model

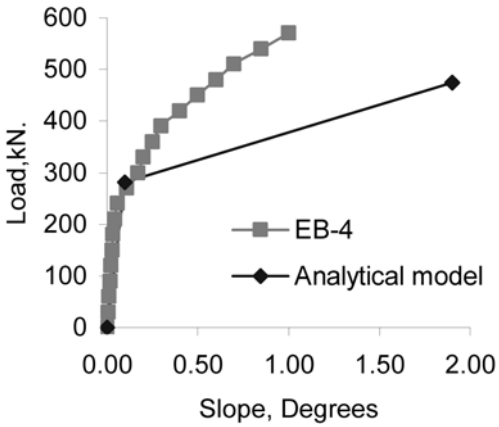

Fig. 23 Slope of the steel bracket during external load for EB-4 and analytical model

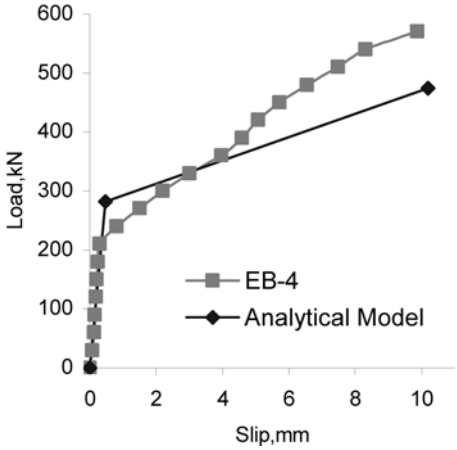

Fig. 24 Slip of the steel bracket during external load for EB-4 and analytical model

Figs. 21 and 22 show the slope and slip of steel bracket for EB-3 and analytical model corresponding to 16 mm dia anchor bolt. Figs. 23 and 24 show the slope and slip of steel bracket for EB-4 and analytical model corresponding to 10 mm dia anchor bolt. From slope and slip of Figs. 21 and 24, it can be observed that the predicted slope and slip values are in good agreement with the experimental observations.

Figs. 25 and 26 show the plot of slope and slip obtained using simple theory and corresponding experimental observations for EB-5. From Figs. 25 and 26, it can be observed that the predicted slope and slip values are in good agreement with the experimental observations.

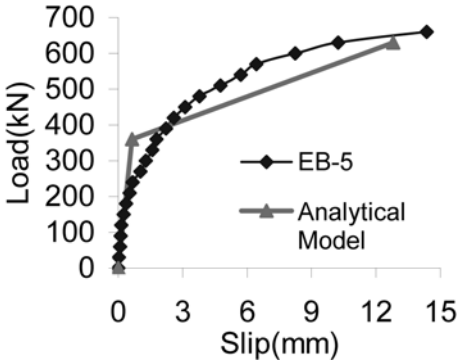

Fig. 25 Slip of the steel bracket during external load for EB-5 and analytical model

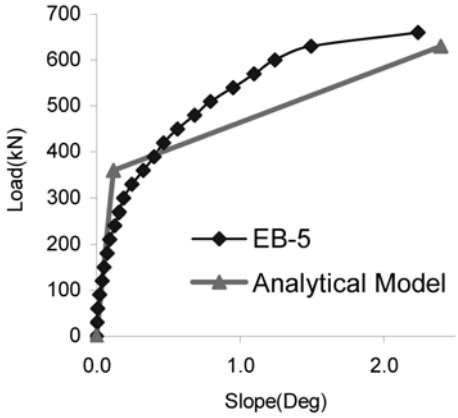

Fig. 26 Slope of the steel bracket during external load for EB-5 and analytical model

5. Conclusions

Details of a novel external prestressing technique for strengthening of concrete members have been presented. In the proposed technique, transfer of external force is in shear mode, on the end block. Steel brackets are provided on either side of the end block for transferring external prestressing force and these are connected to the anchor blocks by expansion type anchor bolts. In order to validate the technique, an experimental investigation has been carried out on post-tensioned end blocks. Performance of the end blocks have been studied for design, cracking and ultimate loads. Slip and slope of steel bracket have been recorded at various stages during the experiment. A ductile failure has been observed in EB-1 where as a sudden failure is observed in EB-4. Finite element analysis has been carried out by simulating the geometry, loading, material nonlinearity and test conditions. Linear and nonlinear static analysis has been conducted for the specified loadings and the responses have been compared. From the analysis, it has been observed that the computed slope and slip of the steel bracket are in good agreement with the corresponding experimental observations. A simplified analytical model has been proposed to compute load-deformation of the loaded steel bracket with respect to the end block. Yield and ultimate loads have been arrived based on force/moment equilibrium equations at critical sections. Deformation analysis has been carried out based on the assumption that the ratio of axial deformation to vertical deformation of anchor bolt would follow the same ratio at the corresponding forces such as yield and ultimate. It is observed that the computed forces, slip and slopes are in good agreement with the corresponding experimental observations.

Acknowledgements

Authors wish to thank Dr Nagesh R. Iyer, Acting Director for his valuable suggestions during the course of investigation. And also wish to thank the staff members of Heavy Testing Laboratory for assisting to conduct the experiments. This paper is being published with the kind permission of the Director, SERC, Chennai.

References

Angel, C. Aparicio, Gonazalo Ramos and Juan R. Casas (2002). Testing of externally prestressed concrete beams. *Eng. Struct.* **24**(1), 73-84.

Angel, C. Aparicio, Gonzalo Ramos, Juan R. Casas (2000). Externally prestressed high strength concrete viaduct, ASCE *J. Bridge Eng.*, **5**(4), 337-343.

ANSYS 6.0 Theory and Reference Manual, 2002.

Ayaho Miyamoto Katsuji Tei, Hideaki Nakamura and John W. Bull (2000). Behavior of prestressed beam strengthened with external tendons. *ASCE J. Struct. Eng.* **126**(9), 1033-1044.

Bahaari, M.R. and Sherbourne, A.N. (2000). Behaviour of eight-bolt large capacity end plate connections. *Comput. Struct.* **77**(3), 315-325.

Choy, S.C., Wong, Y.L., Chan, S.L. (2002). Shear strength of prestressed concrete encased steel beams with bonded tendons. Third International conference on Advances in Steel Structures, *Hong Kong, China,* 543-549.

Christoph Czaderski and Masoud Motavalli (2007). 40-Year-old full-scale concrete bridge girder strengthened with prestressed CFRP plates anchored using gradient method. Composites: *Part. B. Eng.* **38**(7-8), 878-886.

Fanning, P.J., Tucker, M. and Broderick, B.M. (2000). Non-linear finite element analysis of semi-rigid bolted end-plate connections, In: Proc Fifth International Conference on Computational Structures Technology, *Civ. Compress, Edinburgh,* UK, 397-403.

Jung, J.W., Abolmaahi, Ali and Choi, Y. (2006). Finite element analysis of tapered steel and Fiber-Reinforced Plastic Bridge Camera Poles. *ASCE J. Bridge Eng.* 611-617.

Kim, J., Yoon, J.-C. and Kang, B.-S. (2007). Finite element analysis and modeling of structure with bolted joints. *Appl. Math. Model.* **31**, 895-911.

M.A. McNeff P.E. (1999). Calculating service moment capacity of anchor bolted connections. ASCE Practice periodical on Structural Design and Construction, 4CD: 33-35.

Shiming Chen (2005). Experimental study of prestressed steel-concrete composite beams with external tendons for negative moments. *J. Constr. Steel Res.* **61**(12), 1613-1630.

Tie-jiong, Lou and Yi-qiang Xiang (2006). Finite element modeling of concrete beams prestressed with external tendons. *Eng. Struct.* **28**(14), 1919-1926.

Zhongguo (John) Ma, Mohsen A Saleh, Maher K Tadros (1999). Optimized post-tensioning anchorage in prestressed concrete I-beams. *PCI J.,* 56-73.